UC Berkeley
Development and Technology

Title
Modeling Flow and Heat Transfer Through Porous Media for High Heat Flux Applications

Permalink
https://escholarship.org/uc/item/31r8p2jv

Authors
Raffray, A. R.
Pulsifer, J.
Tillack, M. S.

Publication Date
2000-12-01

Energy Development and Technology 002

"MODELING FLOW AND HEAT TRANSFER THROUGH POROUS MEDIA FOR HIGH HEAT FLUX APPLICATIONS"

A.R. Raffray, J. Pulsifer and M.S. Tillack

October 2002

UCEI
University of California Energy Institute

Modeling Flow and Heat Transfer through Porous Media for High Heat Flux Applications

A. R. Raffray*, J. Pulsifer and M. S. Tillack
Fusion Energy Research Program
University of California, San Diego
9500 Gilman Drive
EBU-II, Room 460
La Jolla, CA 92093-0417

*phone: (858) 534-9720; fax: (858) 822-2120; e-mail: raffray@fusion.ucsd.edu

Abstract

Effective heat transfer is essential in a variety of energy technologies in order to enable the maximum possible power density and power conversion efficiency needed for economic competitiveness and fuel conservation. A particularly difficult heat transfer problem exists with gas coolants, due to their inherently low heat capacity and heat transfer coefficient. Innovative techniques have been proposed previously using porous metal heat transfer media infiltrated by the coolant. The general design strategy is to minimize the coolant flow path length in contact with the porous medium, and to minimize the friction factor in that zone while simultaneously maximizing the heat transfer coefficient. In this work we seek to develop improved phenomenological thermal-hydraulic models in order to assess various porous heat transfer media and to help optimize the heat transfer coefficient while minimizing the associated fluid friction in innovative design concepts. The results will be applied to the field of fusion energy research, where extreme thermal conditions exist and gas coolants are favored due to their inherent safety features.

1. Introduction

Fusion power plant studies have found helium to be an attractive coolant based on its safety advantages and compatibility with structural materials at high temperature. The maximum heat flux that can be accommodated is limited by the heat transfer coefficient achievable with flowing helium and the maximum allowable operating temperature of the structural materials. Helium flow through a simple channel provides limited heat transfer performance for fusion-relevant flow rates and pressure; accommodating high heat fluxes requires heat transfer enhancement features.

Porous metal heat exchangers have been studied in the past because of the large surface area they provide for heat transfer. For example, Thermacore has developed a porous metal heat exchanger applicable to fusion plasma-facing components [1,2]. A test article was fabricated and tested in the Sandia National Laboratory electron beam facility where it demonstrated relatively high overall heat transfer coefficients [2,3]. Such a configuration was also considered for the ARIES-ST divertor, as illustrated in Figure 1 [4]. The heat augmentation effect provided by this concept must be evaluated with respect to the associated pressure drop penalty. For a given particle dimension, the pressure drop through a porous medium is highly dependent on the porosity, ε, while the heat transfer coefficient depends more on the specific surface area, S_p. In a conventional particle bed, S_p is directly related to ε through the following equation such that it becomes difficult to optimize the bed characteristics.

$$S_p = \frac{6(1-\varepsilon)}{d_p}$$

(1)

where d_p is the particle diameter.

Minimizing the flow path length as achieved in the concept shown in Fig. 1 does help to some extent to reduce the pressure drop penalty. As shown in Fig. 1, directing the flow through the porous medium around the circumference of the tube instead of along the length of the tube (~150 cm) as in the case of helium flowing in a simple channel, reduces the flow path length for the porous heat exchanger to ~80 mm.

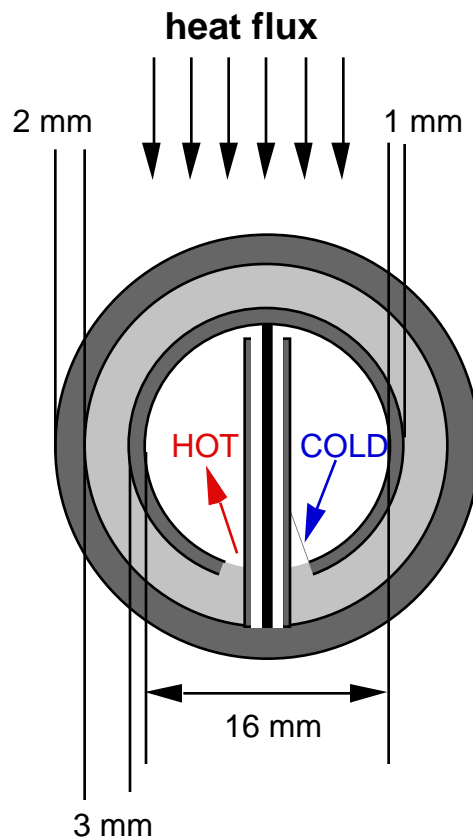Figure 1.   Schematic of a plasma divertor tube with 3-mm porous heat exchanger and inlet and outlet helium headers separated with thermal insulation, proposed for ARIES-ST. The design heat flux normal to the tube is 5 MW/m^2 [4].

An innovative design solution is based on a porous material using non-spherical fibers where the porosity and specific surface area can be optimized beyond their conventional particle bed

dependence. Such a porous foam would have high porosity (which governs the pressure drop) but with specific surface area (influencing the heat transfer) much higher than those that a conventional packed bed can provide. This would open up the window of application of helium for high heat flux fusion applications. Similar foams have been manufactured. For example, Ultramet has proposed a new class of open cell, low density, high-temperature performance refractory foams for a variety of aerospace and industrial applications, as illustrated in Figure 2 [5]. These foams can be fabricated from any material or material combination (either homogeneously combined or layered) which can be deposited by CVD/CVI. Among the materials that can be deposited are the refractory metals, including tungsten, which is particularly useful for fusion applications. These cellular materials can be optimized for various properties (including porosity characteristics) simultaneously, can be furnished in various sizes and configurations, and are easy to machine. Face sheets of either the same or different material can be applied. Such a tungsten foam joined to a tungsten face sheet at the high temperature region and to the structural ferritic steel at the lower temperature region would open the door for higher allowable heat flux for the helium-cooled concept while maintaining the safety advantages of using an inert gas as coolant.
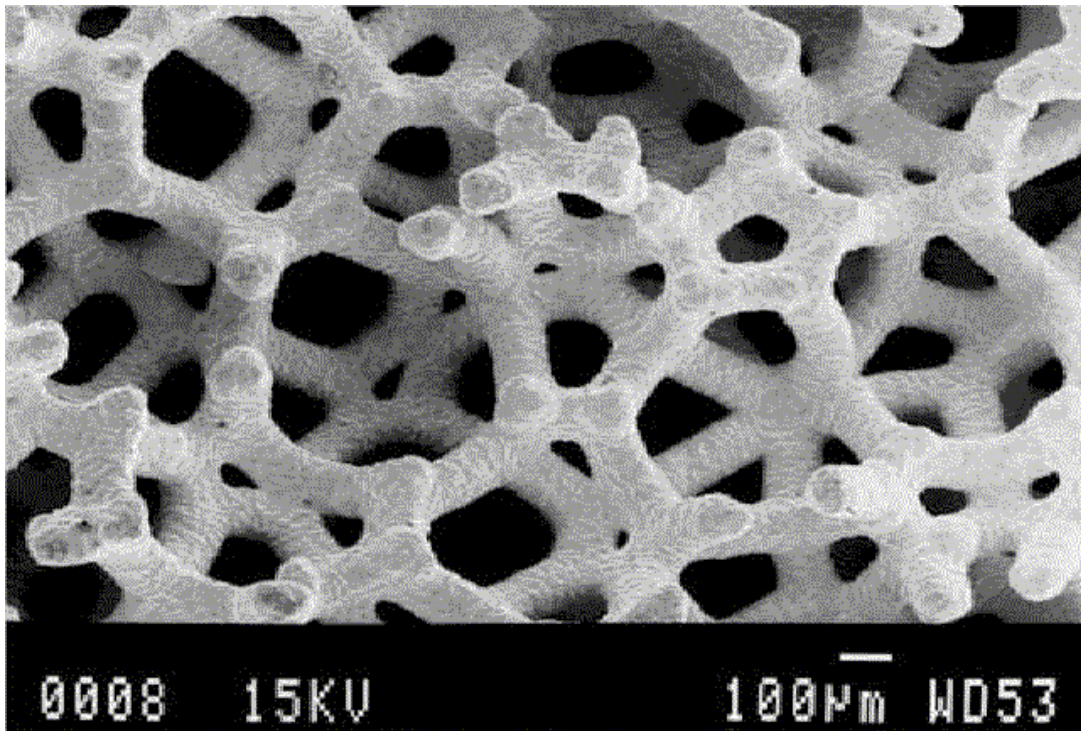

Figure 2   Example of Ultramet refractory foam [5]

This work focused on developing an improved phenomenological thermal-hydraulic model in order to assess and optimize such porous heat transfer media with the intent of guiding the direction of future modeling, material and experimental R&D. The final deliverables are somewhat narrower than what was originally laid out in the proposal which included an assessment of the fabrication possibility of high porosity high specific surface area refractory foams and development of a test program for a test article evolving from the optimization study. However, in order to do justice to the capabilities of the model being developed and to fulfil the letter and spirit of the proposed modeling task, substantially more effort was required in this area than was originally planned. Taking this into consideration as well as the somewhat lower grant budget allocation (~25% lower) than originally requested to complete all tasks, it was decided to focus all effort on the model development and to only perform a preliminary assessment of porous media which could be used as a basis for new proposals to be submitted to various agencies and institutions, and which were quite successful as will be explained in the relevant section.

2. Model Development

Most existing models for heat transfer through a porous media seem to be based on a semi-empirical approach such as the following circuit-based model described in [2].

$$h_{eff} = \left(\varepsilon h_p + \cfrac{1}{R_o + \cfrac{1}{\sqrt{h_p k_p S_p}\ \tanh\left(\sqrt{\dfrac{h_p S_p}{k_p}}\, t \right)}} \right) \tag{2}$$

where h_p is the local particle-to-fluid heat transfer coefficient, R_o is the porous medium/wall interface resistance, k_p is the porous medium thermal conductivity and t is the porous medium thickness.

Such a model provides a useful and convenient means for estimating the overall heat transfer coefficient but is limited in its range of application, e.g. for cases with spatial variation of the microstructure characteristics (e.g. the porosity and directional thermal conductivity). It would be very useful to develop a more comprehensive model to calculate the velocity profile and the corresponding temperature distribution in the porous region with the capability to account for microstructure variation and to include potential important processes such as the local heat transfer between solid and fluid and the effect of dispersion. This was the aim of this work.

The proposed model is called MERLOT :

Model of
Energy-transfer
Rate for
f**L**ow in
Open-porosity
Tailored-media

First, the continuity equation and the modified Darcy equation including Forcheimer's drag term and Brinkman's viscosity term are used in estimating the velocity profile [6]. For fully-developed steady state flow though a 2-D cylindrical geometry (r,) such as shown in Fig. 3, these can be expressed as:

$$\frac{\partial V_\theta}{\partial \theta} = 0 \tag{3}$$

$$0 = -\frac{1}{r}\frac{\partial P}{\partial \theta} - \left(\frac{\mu}{K}\right)V_\theta - \left(\frac{\rho_f C}{\sqrt{K}}\right)V_\theta^2 + \mu_{eff}\frac{\partial}{\partial r}\left(\frac{1}{r}\frac{\partial}{\partial r}(rV_\theta)\right) \tag{4}$$

where V_θ is the superficial velocity in the   direction, P the fluid pressure μ the fluid viscosity; K the porous medium permeability, ρ_f the fluid density, and C the inertia coefficient.
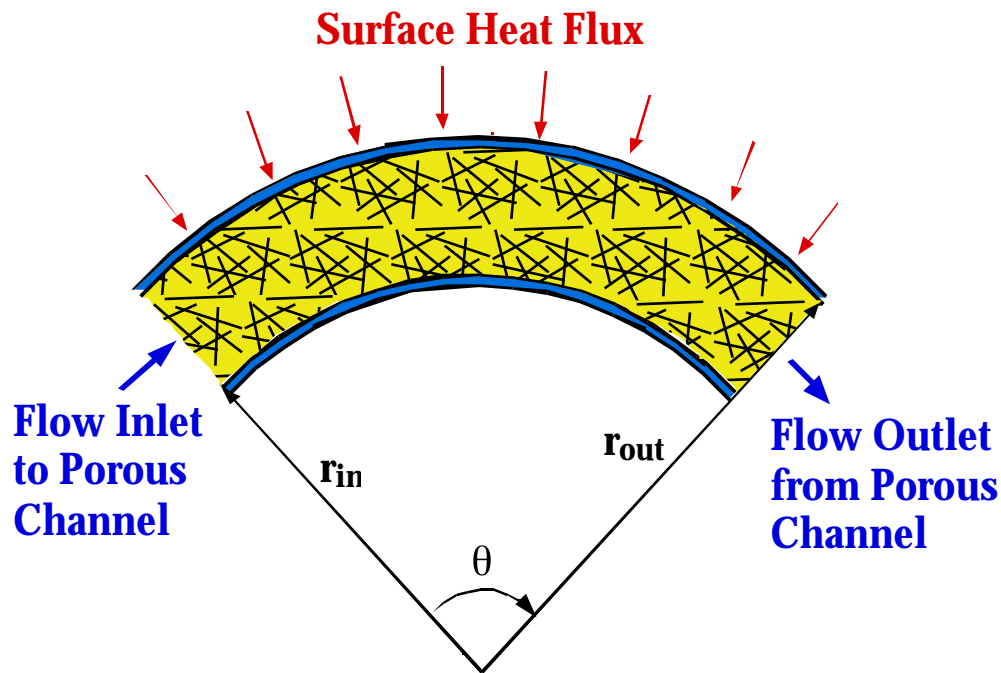

Figure 3   Model geometry for flow through porous media

Eq. (4) can be non-dimensionalized as follows, where the primes refer to non-dimensionalized variables and V_{θ_0} and P_o are the reference Darcy velocity and pressure, respectively.

$$r' = \frac{r}{r_{out}} \tag{5}$$

$$V'_\theta = \frac{V_\theta}{V_{\theta_0}} \tag{6}$$

$$P = \frac{P - P_0}{\rho_f V_{\theta_0}^2} \tag{7}$$

$$0 = -\frac{1}{r'}\frac{\partial P}{\partial \theta} - \frac{V'_\theta}{Re_{ch} Da} - \left(\frac{C V_\theta^2}{\sqrt{Da}}\right) + \frac{1}{Re_{ch}}\frac{\partial}{\partial r'}\left(\frac{1}{r'}\frac{\partial}{\partial r'}(r' V'_\theta)\right) \tag{8}$$

where the Darcy number, Da, and Reynolds number for the channel, Re_{ch} are defined as:

$$Da = \frac{K}{r_{out}^2} \tag{9}$$

$$Re_{ch} = \frac{\rho_f V_{\theta_0} r_{out}}{\mu_{eff}} \tag{10}$$

An implicit finite difference scheme is used to solve Eq. (8) in combination with a tri-diagonal matrix solver subroutine using the Thomas algorithm [7]. The non-dimensional pressure gradient is assumed constant and set as input and the boundary conditions are no slip at both walls (i.e. $V'_{\theta,wall} = 0$). Due to the non-linear velocity term in Eq. (8), an iterative procedure is used to advance the solution by using the old value of velocity to compute the new ones until the desired convergence is reached.

Next, the 2-D temperature distribution can be obtained by separately solving the energy equations for the solid phase and the fluid phase, using a local heat transfer coefficient, h_c, at the interface between solid and fluid [6]. The equations are expressed so as to include the effect of spatial variations of thermal conductivity and porosity.

$$0 = \frac{1}{r}\frac{\partial}{\partial r}\left(r(1-\phi)k_{s,r}\frac{\partial T_s}{\partial r}\right) + \frac{1}{r^2}\frac{\partial}{\partial \theta}\left((1-\phi)k_{s,\theta}\frac{\partial T_s}{\partial \theta}\right) + (1-\phi)q'''_s + h_c S_{BET}(T_f - T_s) \tag{11}$$

$$\rho_f Cp_f \frac{V_\theta}{r} \frac{\partial T_f}{\partial \theta} = \frac{1}{r} \frac{\partial}{\partial r} (r\phi k_{f,t,r} \frac{\partial T_f}{\partial r}) + \frac{1}{r^2} \frac{\partial}{\partial \theta} (\phi k_{f,t,\theta} \frac{\partial T_f}{\partial \theta}) + \phi q''_f + h_c S_{BET}(T_s - T_f) \quad (12)$$

where ϕ is the porosity; $k_{s,r}$ and $k_{s,\theta}$ the solid thermal conductivities in the r and direction, respectively; T_s and T_f the solid and fluid temperatures, respectively; q'''_s and q'''_f the volumetric heat generations in the solid and fluid, respectively; S_{BET} the specific surface area of the porous medium; ρ_f the fluid density; Cp_f the fluid heat capacity; and $k_{f,t,r}$ and $k_{f,t,\theta}$ the total effective fluid thermal conductivities in the r and direction, respectively.

$k_{f,t,r}$ and $k_{f,t,\theta}$ include the fluid thermal conductivity itself (k_f) and the enhancement provided by dispersion effects ($k_{disp,r}$ and $k_{disp,\theta}$) [8].

$$k_{f,t,r} = k_f + k_{disp,r}; \ k_{f,t,\theta} = k_f + k_{disp,\theta} \quad (13)$$

Eqs. (11) and (12) can be non-dimensionalized as follows, where again the primes refer to non-dimensionalized variables and T_h and T_c refer to the cold and hot reference temperatures, respectively. The property data and the heat generation values are all non-dimensionalized by using reference values (denoted with the subscript *ref*).

$$T'_s = \frac{T_s - T_c}{T_h - T_c} \ ; \ T'_f = \frac{T_f - T_c}{T_h - T_c} \quad (14)$$

$$k'_s = \frac{k_s}{k_{s,ref}} \ ; \ k'_f = \frac{k_f}{k_{f,ref}} \quad (15)$$

$$\rho'_f = \frac{\rho_f}{\rho_{f,ref}} \quad (16)$$

$$Cp'_f = \frac{Cp_f}{Cp_{f,ref}} \quad (17)$$

$$q'_s = \frac{q'''_s}{q'''_{ref}} \ ; \ q'_f = \frac{q'''_f}{q'''_{ref}} \quad (18)$$

$$h'_{eff} = \frac{h_c S_{BET}(T_h - T_c)}{q'''_{ref}} \quad (19)$$

The following parameters, J_s, $J_{f,1}$ and $J_{f,2}$ are introduced to simplify the equation display:

$$J_s = \frac{k_{s,ref}(T_h - T_c)}{r_{out}^2} \tag{20}$$

$$J_{f,1} = \frac{k_{f,ref}(T_h - T_c)}{r_{out}^2} \tag{21}$$

$$J_{f,2} = \frac{\rho_{f,ref} Cp_{f,ref} V_{\theta_0}(T_h - T_c)}{r_{out}} \tag{22}$$

$$0 = J_s(\frac{1}{r'}\frac{\partial}{\partial r'}(r' k'_{s,r}(1-\phi)\frac{\partial T'_s}{\partial r'}) + \frac{1}{r'^2}\frac{\partial}{\partial \theta}(k'_{s,\theta}(1-\phi)\frac{\partial T'_s}{\partial \theta})) + (1-\phi)q'''_{ref} q''_s + q''_{ref} h'_{eff}(T'_f - T'_s) \tag{23}$$

$$J_{f,2}\rho'_f Cp'_f \frac{V'_\theta}{r'}\frac{\partial T'_f}{\partial \theta} = J_f(\frac{1}{r'}\frac{\partial}{\partial r'}(r' k'_{f,t,r}\phi\frac{\partial T'_f}{\partial r'}) + \frac{1}{r'^2}\frac{\partial}{\partial \theta}(k'_{f,t,\theta}\phi\frac{\partial T'_f}{\partial \theta})) + \phi q''_{ref} q'''_f + q'''_{ref} h'_{eff}(T'_s - T'_f) \tag{24}$$

Although the above equations are expressed in general terms to include the effect of porosity variation in both r and   directions, in the geometry of interest represented in Fig. 1, the porosity will only vary with r but not with   .

Eqs. (23) and (24) are solved based on an implicit alternating direction finite difference scheme using the velocity distribution from the solution of Eq. (8) as input and based on the following boundary conditions[7]:

- At inlet, $\theta = 0$, the temperature is set at the uniform inlet temperature; and
- At outlet, $\theta = \theta_{out}$ for simplicity, adiabatic conditions are assumed.
- At both walls, r=r$_{in}$ and r=r$_{out}$, the boundary conditions are set by equating the total heat flux, q''_w to the combined fluid and solid heat fluxes. For example, for the inner wall the boundary condition is:

$$(q'_w = -(1-\phi)k_{s,r}\frac{\partial T_s}{\partial r} - \phi k_{f,t,1}\frac{\partial T_f}{\partial r})_{innerwall} \tag{25}$$

$k_{f,t,1}$ in the equation represents an effective conductivity for the fluid at the wall including a convection component averaged over the radial increment at the wall.

Eq. (25) can be written in non-dimensional form as follows:

$$(q'_w q''_{w,ref} = -\frac{(T_h - T_c)}{r_{out}}((1-\phi)k_{s,ref}k'_{s,r}\frac{\partial T'_s}{\partial r'} - \phi k_{f,ref}k'_{f,t,1}\frac{\partial T'_f}{\partial r'})_{innerwall} \qquad (26)$$

where the wall heat flux is non-dimensionalized based on a reference value:

$$q'_w = \frac{q''_w}{q''_{w,ref}} \qquad (27)$$

The solution proceeds iteratively. First, tri-diagonal matrix equations for the temperature in the r direction along each successive theta plane are solved using the old temperature values in the theta direction terms. Next, similar tri-diagonal matrix equations but for the temperature along the theta direction are solved using the just computed temperature values in the r-direction. The program iterates in these alternating direction solutions until the desired convergence is achieved.

3. Model Validation

The model seemed to provide consistent and qualitatively correct results for both the velocity profiles and temperature profiles based on expected results for given porosity variations. It was difficult to find from the literature results for curved geometry for final confirmation of the results. An example set of results that were found were from Cheng and Hsu who considered the variation in porosity for a packed-sphere bed and calculated the wall channeling effect on axial velocity for an annular geometry with flow in the axial direction and assuming only the Brinkman viscous effect but not the Forcheimer inertial effects [9]. They used the following expressions to estimate the porosity variation:

$$\phi = \phi_{inf}(1 + C_1 \exp(-N_1 \frac{(r_{out} - r)}{d_p})) \qquad \text{for } 0.5(r_{out} - r_{in}) \quad r \quad r_{out} \qquad (28)$$

$$\phi = \phi_{inf}(1 + C_1 \exp(-N_1 \frac{(r - r_{in})}{d_p})) \qquad \text{for } r_{in} \quad r \quad 0.5(r_{out} - r_{in}) \qquad (29)$$

where C_1=1 and N_1=2 for a bulk porosity, ϕ_{inf} of 0.4 [9].

For a particle bed, consistent with the Ergun and Kozeny equations, the permeability is given by [6,8]:

$$K = \frac{d_p^2 \varphi^3}{A(1-\varphi)^2}$$
(30)

where A is a shape factor (=150).

MERLOT was run with a large aspect ratio over a short angle to simulate flow in a straight channel for conditions similar to those used in Ref. [9] including the above porosity and permeability equations, and setting the inertia coefficient, C=0 in eq. (4) to exclude the Forcheimer effect. The resulting velocity profiles compared reasonably well with Cheng and Hsu's results given the inherent differences in geometry, as illustrated in Fig. 4 for a case with a $\frac{d_p}{r_{in}}$ of 0.085.
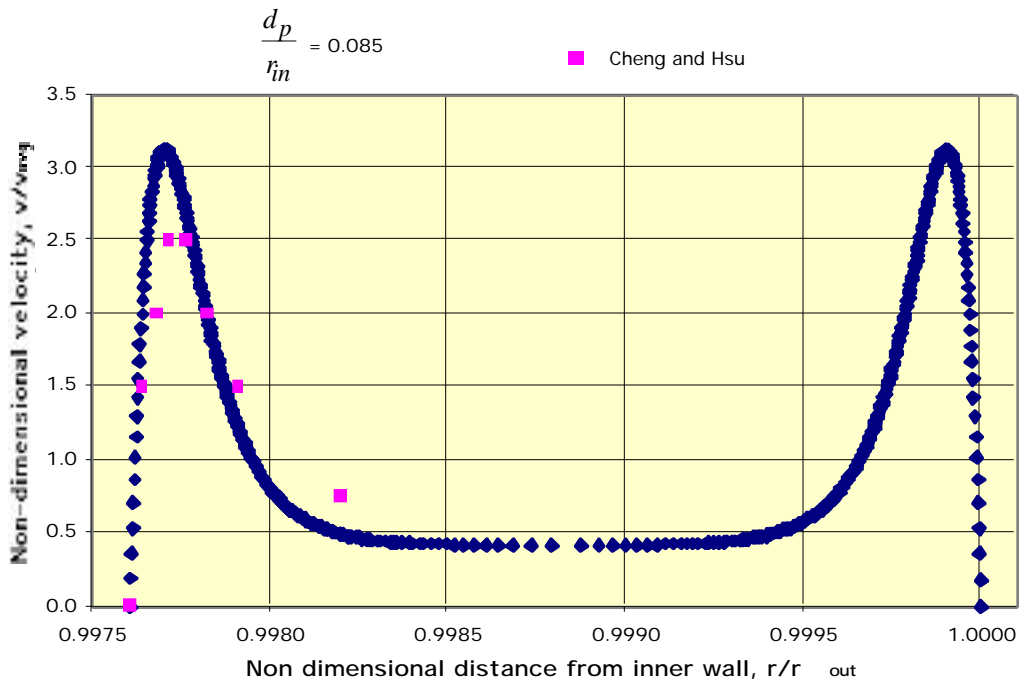

Figure 4   Comparison of velocity profile computed from MERLOT to the results from Cheng and Hsu [8]

The energy part of the code was validated by comparing the temperature distribution for simple cases involving heat fluxes at the wall or heat generation in the solid to predicted profiles. Also, conservation of energy was verified for a number of set cases to ascertain the code robustness in analyzing cases with different geometries, heat inputs, and porous microstructure. This was

assessed by comparing the energy transferred to the coolant between inlet and outlet to the energy input either through the wall heat flux or volumetric heat generations. In all cases an energy balance was achieved to a reasonable level (within a few %) by refining the mesh and convergence criterion.

4. Example Parametric Study

An example parametric study was performed for a typical case corresponding to the ARIES-ST divertor and the dimensions shown in Fig. 1 [4]. The model considered the top half of the tube ($=0$ to $=$) subjected to a 5 MW/m^2 heat flux. Other parameters were set as shown in Table 1.

Table 1   Parameters used for parametric study

Fluid	He
Fluid properties	Varied as f(T)
Reference solid thermal conductivity	100 W/m-K
Particle diameter	0.2 mm
Bulk porosity	0.4
Porosity variation	Based on eqs. (28) and (29
Inner radius	9 mm
Outer radius	12 mm
He inlet temperature	350 °C

For simplicity, in these example calculations, no thermal dispersion effect was assumed and convections between solid and fluid at the wall and in the bulk were assumed very high.

The calculations proceeded as follows:

1.   The approximate He outlet temperature desired for the design was set (650°C).
2.   The He mass flow rate corresponding to the He temperature rise and the heat input was calculated.
3.   The pressure gradient, $\frac{dP}{dx}$, corresponding to the He mass flow rate, the average porosity and the particle diameter was estimated from the well-known Ergun equation for a packed bed [1,6].

$$\frac{dP}{dx} = 150 \frac{(1-\varepsilon)^2}{\varepsilon^3} \frac{\mu_f V_0}{(\varphi d_p)^2} + 1.75 \frac{(1-\varepsilon)}{\varepsilon^3} \frac{\rho_f V_0^2}{\varphi d_p} \tag{31}$$

where μ_f is the fluid viscosity; V_0 the superficial velocity, φ = particle shape factor, and ρ_f the fluid density. This expression implies an inertia coefficient, C, given by:

$$C = \frac{1.75(1-\varphi)}{\varphi^3 d_p} \tag{32}$$

4. The correct velocity profile corresponding to this pressure gradient and to the porosity spatial distribution was then computed.

5. Finally, the corresponding 2-D temperature distribution in the solid and fluid was calculated, yielding the exact He outlet temperature.

Figure 5 shows an example of the temperature distribution in the porous media obtained from the results. The temperature gradient in the radial direction is governed by heat diffusion from the heat flux at the outer wall, the total heat input dictating the temperature rise along the flow direction ( ) with, as expected, an inlet temperature of 350°C and an outlet temperature of ~ 650°C.

The effect on the heat transfer performance of varying the solid thermal conductivity was determined and the results are illustrated in Figure 6. The maximum outer wall temperature (at the outlet) is used as an inverse measure of the heat transfer performance and can be seen to rise at an increasing rate as the solid thermal conductivity is decreased. Clearly, high solid conductivity is a key porous media requirement for high heat flux application in particular since there is no adverse effect on the fluid flow associated with change in this parameter.
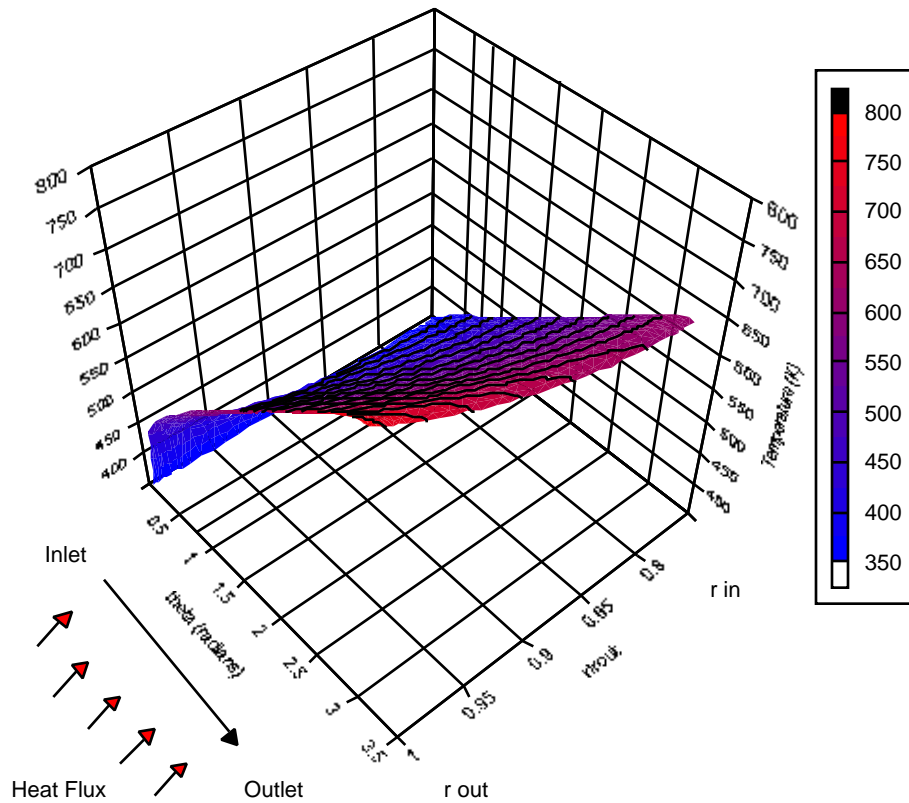
Figure 5   Temperature distribution in porous bed channel for a bulk porosity of 0.4 and a
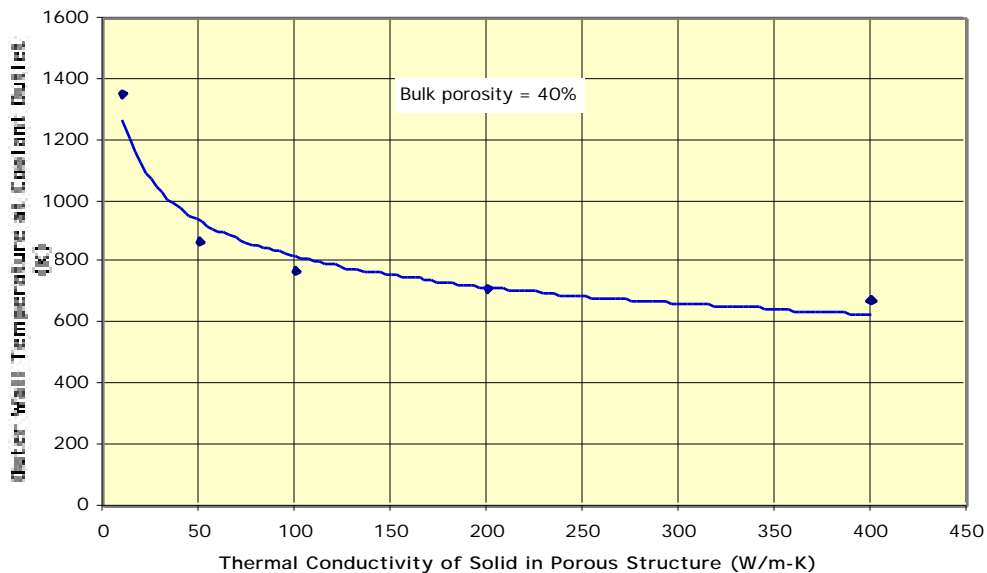solid thermal conductivity of 100 W/m-K

Figure 6   Outer wall temperature at coolant exit as a function of porous bed solid
thermal conductivity

The effect on the heat transfer performance of varying the packed bed bulk porosity was also investigated. For the parameters listed in Table 1, the maximum outer wall temperature (at the outlet) decreases from 770 °C for a bulk porosity of 0.4, to 750 °C for a bulk porosity of 0.3, to 742°C for a bulk porosity of 0.25. Lowering the porosity does produce a somewhat better heat transfer performance but the improvement is not very significant in this example case particular when considering that this will be accompanied by a substantial increase in pressure drop, as illustrated in Figure 7. Clearly, the packed bed is limited in terms of the benefit in improved heat transfer that it provides relative to the high pressure drop penalty. This confirms strongly that the microstructure of porous media for high heat flux application must be carefully designed well beyond those of the conventional packed bed for attractive performance.
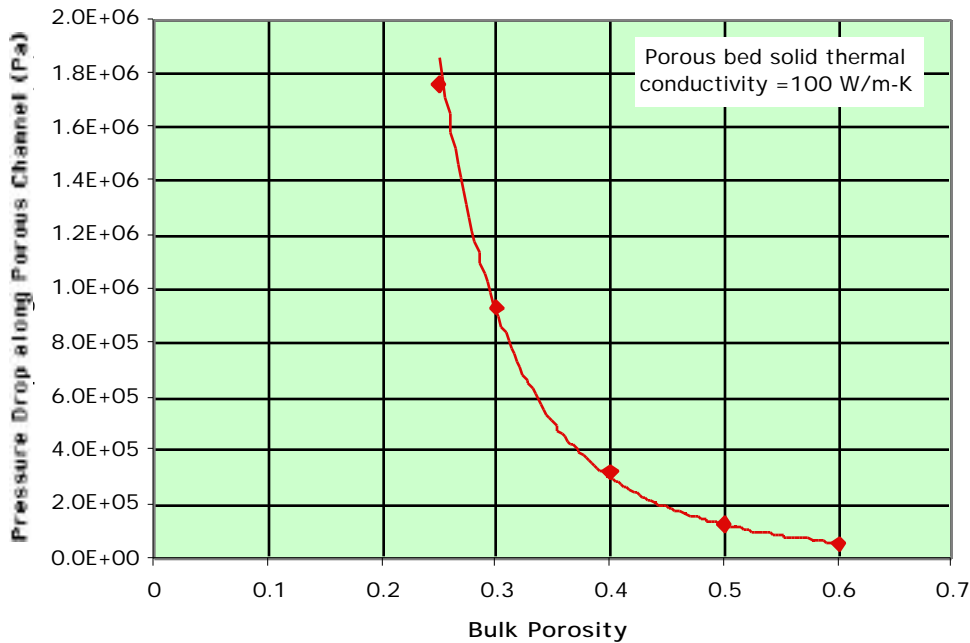

Figure 7   Pressure drop along porous channel as a function of bulk porosity

5. Future Work

The initial efforts in this area are very encouraging. The MERLOT computer code is now running very well and, as reported above, has already been used to do some initial parametric studies. Future effort will include:

- Better characterization of the heat transfer coefficients at the wall and between the solid and fluid in the porous structure, and parametric assessment of their effects on the heat transfer performance of the porous media.

- Inclusion of permeability factor for non spherical porous medium in order to help optimize microstructure geometry for better heat transfer experience

The initial work and results provide a good basis for writing proposals for a more extensive effort in this area.

References

1. J. H. Rosenfeld, "Porous Metal Heat Exchanger for Cooling Plasma-Facing Components", DoE SBIR Phase I Final Report, DE-FG05-92ER81645, June 1994.

2. J. H. Rosenfeld, J. E. Toth, and A. L. Phillips, "Emerging Applications for Porous Media Heat Exchangers", Proc. Int. Conf. on Porous Media and their Applications in Science, Kona, Hawaii, June 1996.

3. D. L. Youchison, M. G. Izenson, C. B. Baxi, J. H. Rosenfeld, "High Heat Flux Testing of Helium-Cooled Heat Exchangers for Fusion Applications", Fusion Technology, Vol. **29** (no.4) July 1996, p.559-570.

4. M. S. Tillack, X. R. Wang, J. Pulsifer, S. Malang, D. K. Sze, M. Billone, I. Sviatoslavsky, and the ARIES Team, "Fusion power core engineering for the ARIES-ST power plant," submitted for publication in Fusion Engineering and Design, 1999.

5. Andrew J. Sherman, Robert H. Tuffias, and Richard B. Kaplan, "Refractory Ceramic Foams: A Novel New High Temperature Structure", http://www.ultramet.com/foamtech.htm, 1999. See also A. J. Sherman, B. E. Williams, M. J. DelaRosa, and R. LaFerla, "Characterization of Porous Cellular Materials Fabricated by CVD," presented at the 1990 MRS Fall Meeting, Boston, MA, 26-30 November 1990.

6. D. A. Nield and A. Bejan, "Convection in Porous Media," 2nd edition, Springer, New York, 1999.

7. D. A. Anderson, J. C. Tannehill and R. H. Pletcher, "Computatiuonal Fluid Mechanics and Heat Transfer," Hemisphere Publishing Corporation, New York, 1984.

8. C. T. Hsu and P. Cheng, "Thermal Dispersion in Porous Medium," Int. J. Heat Mass Transfer, Vol. 33, No. 8, pp1587-1597, 1990.

9. P. Cheng and C. T. Hsu, "Fully-Developed, Forced Convective Flow through an Annular Packed-Sphere Bed with Wall Effects," Int. J. Heat Mass Transfer, Vol. 29, No. 12, pp1843-1853, 1986.